Progress In Electromagnetics Research Letters, Vol. 96, 37–45, 2021

A Novel Miniaturized Circularly Polarized Antenna with Shorting Pins and Parasitic Strips for BeiDou Satellite Navigation System Applications

Ya-Bing Yang[1, 2, *], Fu-Shun Zhang[1], and Mu-Zhao Zheng[2]

Abstract—In this paper, a novel miniaturized circularly polarized (CP) antenna for BeiDou Satellite Navigation System (BDS) applications is presented. The proposed antenna is composed of three substrates with the same size, which are combined by four shorting pins. Parasitic strips are used to reduce the size, and the radiation patch is fed by two coupling feeding patches with the same amplitude and 90° phase difference. The overall dimension of the proposed antenna is only 18 mm × 18 mm × 23.5 mm (about $0.08\lambda_0 \times 0.08\lambda_0 \times 0.1\lambda_0$), and its weight is about 25 grams. The performance study with different geometric parameters has been conducted. A prototype based on optimized dimensions has been fabricated and measured, and the tested results exhibit a good impedance matching bandwidth ranging from 1.2 to 1.35 GHz centered at 1.268 GHz. This antenna also has stable hemispherical radiation patterns and good CP characteristics. Good agreement between analytical and experimental results is obtained.

1. INTRODUCTION

In recent years, satellite navigation systems have been intensively used in various fields. Many countries have developed their own systems, such as GPS, Galileo, and GLONASS [1]. The BDS has been independently constructed and operated by China with an eye to the needs of the country's national security, economic and social development. It is planned to complete the BDS-3 deployment with the launching of 30 satellites by around 2020 to provide services to global users [2]. One of the representative frequencies for the BDS is the B3 band of 1268.52 ± 10.23 MHz, and this bandwidth is relatively narrow. For the terminal application of this system, such as handheld devices, good CP performance and hemispherical widebeam pattern are necessary, and it should also have the performance of miniaturization, light weight, and easy processing [3].

There are many techniques for realizing antenna size reduction. Using high permittivity materials is the simplest way. However, this method's drawbacks are narrow bandwidth, substantial thickness, and expensive cost [4]. Metamaterial could also be used in antenna design. Electromagnetic bandgap structures (EBG), artificial magnetic conductor (AMC), and reactive impedance surfaces (RIS) are commonly used to enhance the antenna performance and significantly reduce the antenna size [5, 6]. Such kind of antennas employing metamaterial have broad application prospects in modern satellite communications. Despite the drawbacks of complex construction and great difficulty in processing, it also increases the back radiation and weakens the antenna gain. For the patch antenna and planar folded dipole, their size can also be effectively reduced by meandering the radiator. This method is realized by prolonging the duration current along the curves; therefore, the surface of the radiation patch

Received 6 October 2020, Accepted 13 January 2021, Scheduled 26 January 2021

* Corresponding author: Ya-Bing Yang (antenna206@163.com).

[1] Key Laboratory of Antennas and Microwave Technology, Xidian University, Xi'an, Shaanxi 710071, China. [2] Xi'an Electronic Engineering Research Institute, Xi'an, Shaanxi 710100, China.

can be reduced [7–11]. However, it leads to poor polarization purity and directional characteristics. Embedding tails along the edges or cutting slots on the driven patch has been investigated for antenna size reduction [12, 13]. The approach provides inductive and capacitive (LC) loading to the radiation patch, but the size reduction is not very effective. Adding shorting pins or shorting walls is one of the most prominent solutions for miniaturized antenna design, in theory which can reduce the size by about half. The antenna miniaturised by utilizing a combination of split-ring resonators and reactive pin loading reduce the electrical size of the antenna diameter by 44% [14]. Meanwhile, the shorting pins caused nearly none performance degradation. The technique can also be applied in single band, wideband, or multiband patch antenna [15].

Some other researches on miniaturized antenna by employing parasitic shorting strips, which operate as an LC loading, have obtained impressive reduction on the size of radiation patch. A small printed patch antenna with four parasitic short-circuited L-shaped strips is utilized for antenna size reduction with broad beamwidth [16]. A CP four-element sequential-rotation array antenna has realized dual-band operation and miniaturized size by adopting a radiation-coupled dual-L structure and parasitic elements [17]. By loading capacitive strips on the corner-truncated patch, a CP antenna obtained about 56% size reduction [18]. A similar technology has been used in [19]. The comparison with previous works is listed in Table 1.

Table 1. Comparison to previous antennas (λ_0 is wavelength of center frequency).

	Overall Size (λ_0)	**HPBW (°)**	**BW (%)**
[3]	$0.13 \times 0.13 \times 0.07$	170	5.9
[4]	$0.33 \times 0.33 \times 0.07$	101	21.3
[7]	$0.17 \times 0.17 \times 0.13$	112	2.3
[12]	$0.35 \times 0.35 \times 0.03$	-	6.4
[16]	$0.17 \times 0.17 \times 0.03$	-	3.2
This work	$0.08 \times 0.08 \times 0.1$	140	11.8

In this article, a novel miniaturized CP antenna for BDS applications has been accomplished by integrating shorting pins and parasitic strips at the four corners of the radiation patch. Parametric studies are also carried out to investigate the effects of key physical dimensions. A prototype was fabricated and tested to validate the design, achieving a very good agreement between the simulated and measured results, which show that the proposed antenna obtained a bandwidth (AR < 3 dB and $|S_{11}| < -10$ dB) over 11.8% corresponding to the center frequency of 1.268 GHz. Besides, there is a significant increase in the half power beamwidth (HPBW) compared with traditional CP antenna.

2. ANTENNA DESIGN AND ANALYSIS

For the purpose of size reduction, shorting pins are widely used in antenna design. Although this method can effectively reduce the whole size, a higher level of cross polarization is normally exhibited due to the asymmetric structure. This defect could be conquered by these shorting pins placed symmetrically. This section presents the design and analysis of the proposed miniaturized CP antenna.

2.1. Design of the Proposed Antenna

The geometry and configuration of the proposed antenna is depicted in Fig. 1. As seen, four shorting pins are introduced for antenna size reduction. To generate the CP radiation, two orthogonal modes with 90° phase differences are required. The antenna is dual-fed with two feeding pins connecting to the feeding network at the bottom of the whole structure. Four open slots are etched at the four corners of the radiation patch, and four parasitic strips are introduced inside these slots. The use of parasitic strips provides an LC loading to the radiation patch and thus increases the effective resonant length.

The proposed antenna is composed of three substrates. Substrate 1 is the radiation body with dielectric constant of 3.5 and thickness of 1.5 mm. Substrate 2 is a metal plane with thickness of 1 mm. Substrate 3 is the feeding network, designed on Rogers TMM 10i ($\varepsilon_r = 9.8$, $H_3 = 1$ mm). The feeding patches are printed on the top surface of substrate 1, with feeding pins connecting to the feeding network. The air gap with height of $H_4 = 20$ mm is employed between the radiation patch and metal ground plane. For structural strength, this gap is filled with poly foam when this antenna is fabricated. All the dimensions are marked in Figs. 1 and 2, and listed in Table 2 in detail.

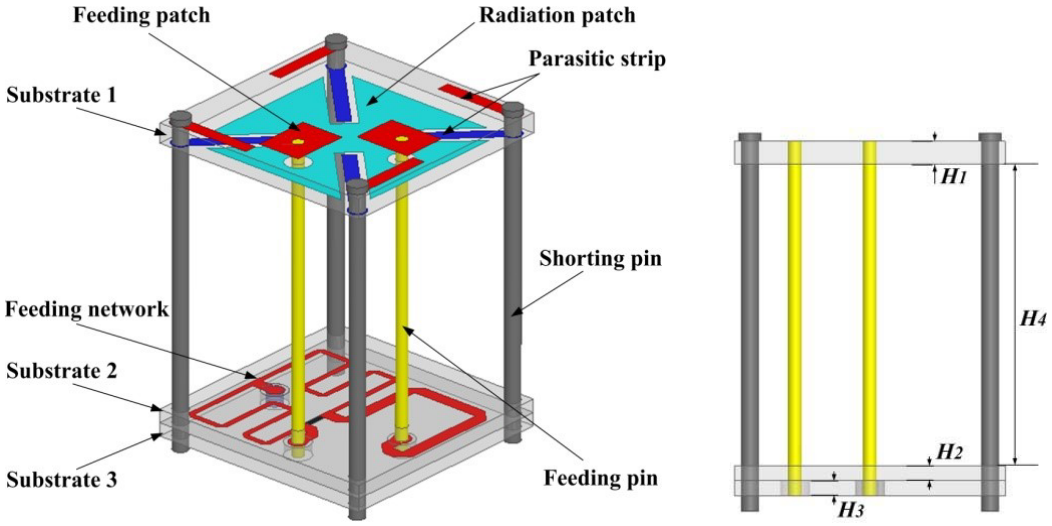

(a) Perspective view (b) Side view

Figure 1. Geometry and configuration of the proposed antenna.

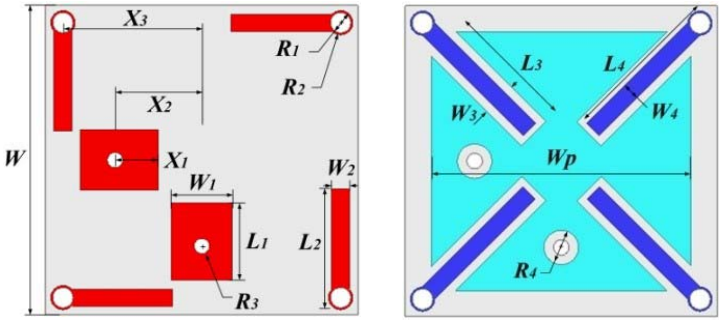

(a) Top layer (b) Bottom layer

Figure 2. Top and bottom layers of the Substrate 1.

In order to demonstrate that the size of the proposed antenna can be further reduced by using the parasitic strips, the current distributions on the shorting pins with and without the parasitic strips are analyzed. As depicted in Fig. 3, it can be seen that the strongest current strength (the red arrow) concentrates at the shorting pins with the parasitic strips added, and nearly no current is observed on the antenna without parasitic strips.

2.2. Design of the Feeding Network

As the proposed antenna is dual-fed, its two feeding ports are of the same amplitude and 90° phase difference. The feeding network is composed of an equal Wilkinson power divider and 90° phase shifter,

Table 2. Dimensions of the proposed antenna (Unit: mm).

W	W_1	L_1	W_2	L_2	W_3	L_3
18	3.5	4.5	1	7	2	7.5
W_4	L_4	W_P	H_1	H_2	H_3	H_4
1	9.5	15	1.5	1	1	20
X_1	X_2	X_3	R_1	R_2	R_3	R_4
2.5	5	8	1.2	1.4	0.9	2

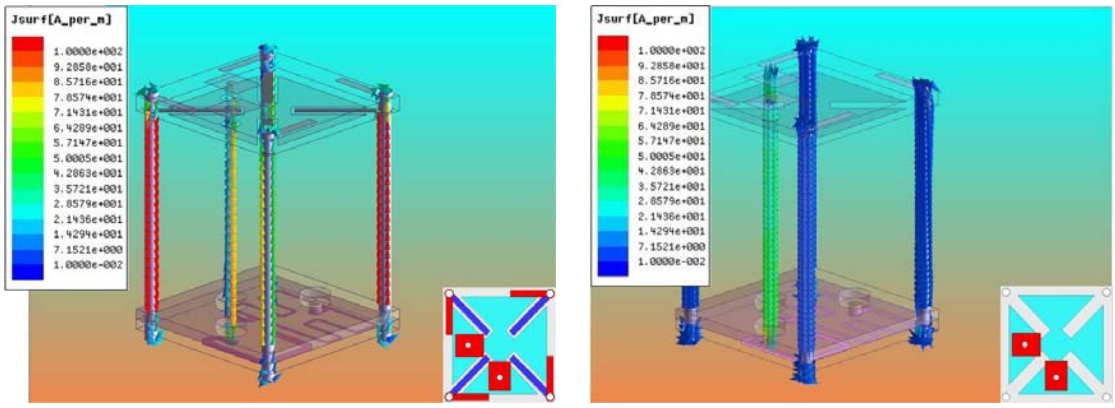

(a) with parasitic strips (b) without parasitic strips

Figure 3. The current distribution with or without parasitic strips.

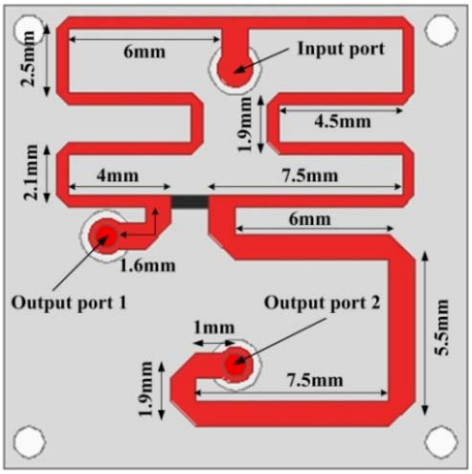

Figure 4. Detail dimension of the feeding network.

as depicted in Fig. 4. In order to reduce the whole size of antenna, the feeding network is printed on a high permittivity substrate. The input port is combined with an sub-miniature-A (SMA) connector, and these two output ports are connected to the feeding patch with metal feeding pins. The microstrip lines are curved for compact arrangement. All the dimensions of the feeding network are marked in Fig. 4.

The simulated results of the feeding network are shown in Figs. 5 and 6, and the simulated frequency

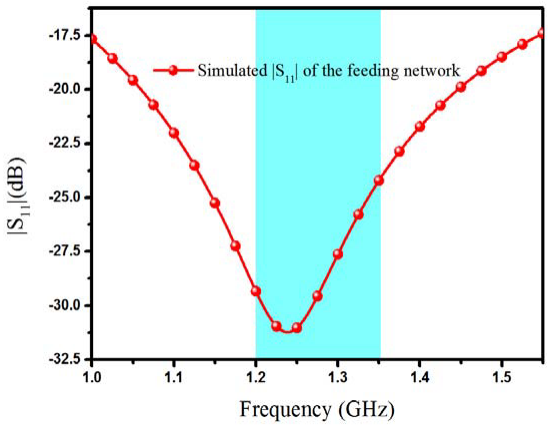

Figure 5. Simulated return loss of the feeding network.

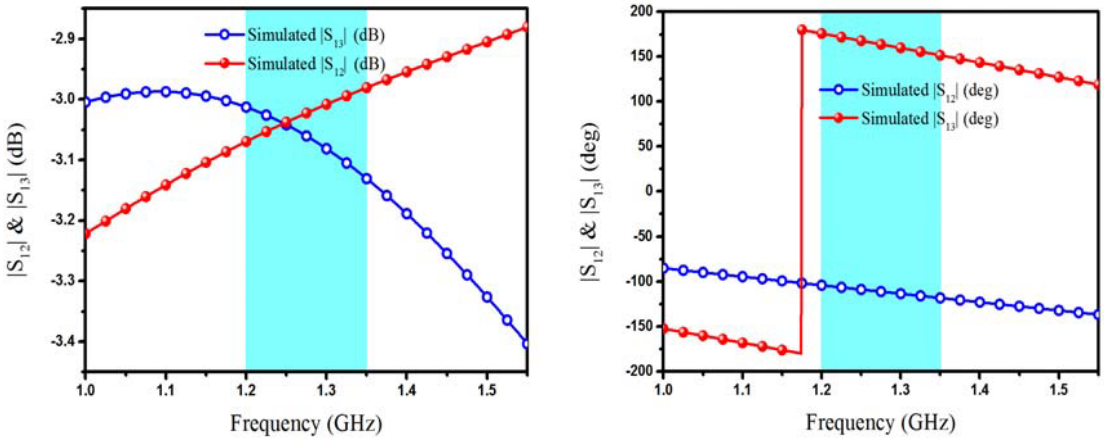

(a) Amplitude (b) Phase

Figure 6. Simulated amplitude and phase of the feeding network.

band is from 1.0 GHz to 1.55 GHz. As shown in Fig. 5, $|S_{11}|$ is below -17 dB within the whole band. The dark area represents the operation band of the proposed antenna. The result shows that the feeding network is well matched.

The simulated amplitude and phase of these two output ports are depicted in Fig. 6. The amplitude difference is less than 0.15 dB in the dark area, and the phase difference is between 89.2° and 91.0°. The simulated results indicate that the proposed feeding network owns excellent performance.

2.3. Parametric Studies and Analysis

Parametric studies have been done to investigate the effects of key parameters on the return loss and radiation patterns. Rigorous simulations indicate that the resonance frequency and radiation performance are mainly determined by the length of parasitic strip (L_2 & L_4), the height of the air gap (H_4), and the width of radiation patch (W_p). To obtain a good understanding, only one parameter is investigated at a time, while the others are kept fixed.

Based on the principle of the proposed antenna, the resonance frequency is mainly determined by the length of parasitic strip combined with the shorting pins, which determines the path of surface current. As there are two sets of parasitic shorting strips, the lengths of L_2 and L_4 are studied respectively. Fig. 7(a) illustrates the simulated $|S_{11}|$ for different values of L_2 varied from 6.6 mm to 7.4 mm. It is noted that the impedance matching changes obviously with the length of parasitic strip (L_2). And the

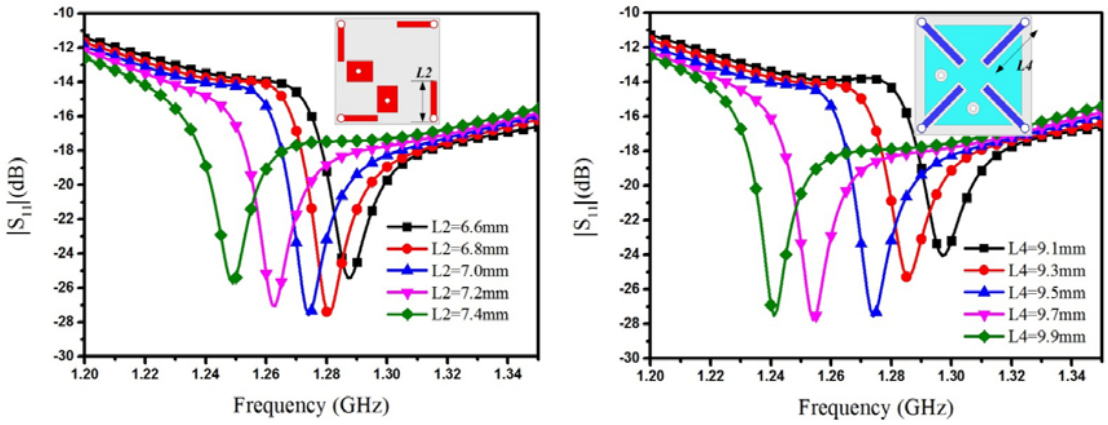

(a) Parameter L_2 (b) Parameter L_4

Figure 7. Simulated return loss varies with different parameters.

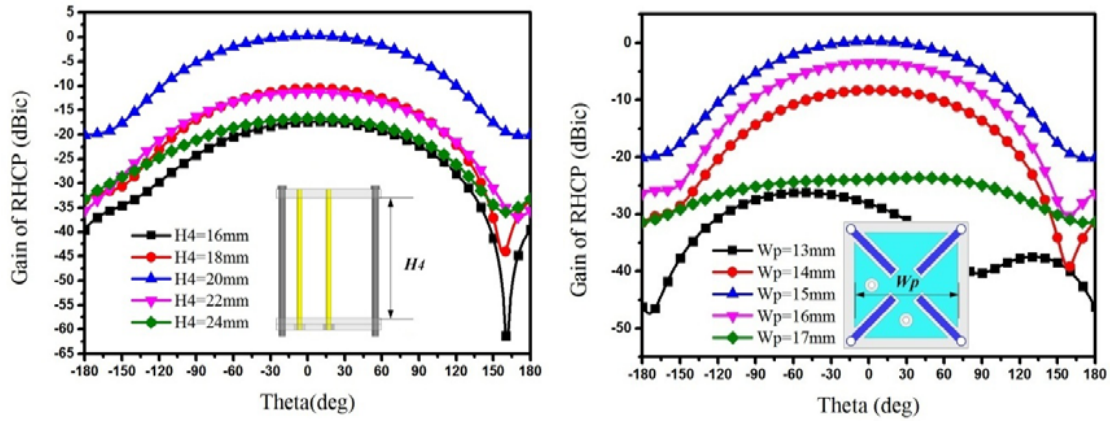

(a) Parameter H_4 (b) Parameter W_P

Figure 8. Simulated radiation patterns varies with different parameters.

resonance frequency is shifted to lower frequencies with the increase of this parameter. When L_2 equals 7 mm, the proposed antenna operates at the BDS B3 band. The length of the parasitic shorting strip (L_4) has a similar effect, as depicted in Fig. 7(b).

The effect of air gap to the simulated right hand circularly polarized (RHCP) gain is also studied. As shown in Fig. 8(a), the simulated RHCP radiation patterns are varied with H_4 from 16 mm to 24 mm have been presented. It can be seen that the RHCP radiation characteristics are significantly affected by the height of air gap (H_4). Apparently, the case of 20 mm is the proposed optimal design, which is only about $0.08\lambda_0$. Furthermore, the simulated gain for the width of the radiation patch W_p varied from 13 mm to 17 mm is depicted in Fig. 8(b). Obviously, the dimension of the radiation patch is another key parameter. With this parameter adjusted precisely, the proposed antenna would operate at 1.268 GHz with a good RHCP radiation feature.

The simulated radiation patterns of the antenna with optimized parameters at 1.268 GHz are presented in Fig. 9, which are symmetric with respect to the boresight. As seen, the proposed antenna exhibits a bidirectional pattern, and the cross-polarization level is more than 20 dB at the boresight. In addition, the HPBW is about 140°, the wide-beam pattern is one of the most attractive performances for the antenna used in navigation systems.

The simulated results above clearly indicate that these parameters have great effects on the resonant frequency, radiation patterns, and peak gain. On reviewing this whole process, the introduction of

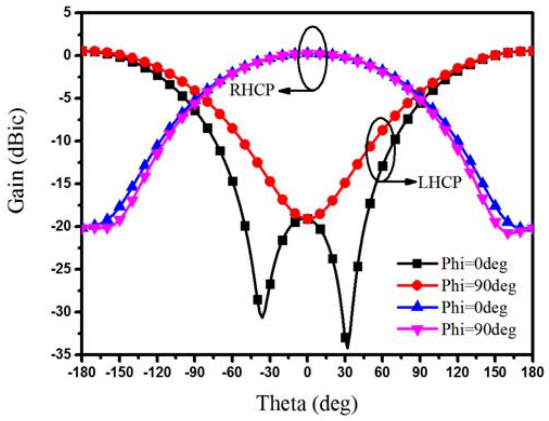

Figure 9. Simulated radiation patterns at 1.268 GHz.

parasitic strips enables the antenna radiate normally at 1.268 GHz. Thus, the proposed antenna can be used for BDS applications that require wide beamwidth and RHCP radiation characteristics with less constraints on the size and weight.

3. RESULTS AND DISCUSSION

To validate the proposed design, a prototype of the proposed antenna based on the simulated model has been fabricated, and its photographs are shown in Fig. 10. The return loss measurement was carried out by using Agilent N5244A network analyzer, while the radiation characteristics were measured with the antenna far-field measurement system in a microwave anechoic chamber at Xi'an Electronic Engineering Research Institute, Shaanxi, China. When the proposed CP antenna was under test, it worked as a transmitter, and a probe with the same operation band was used to receive the signal.

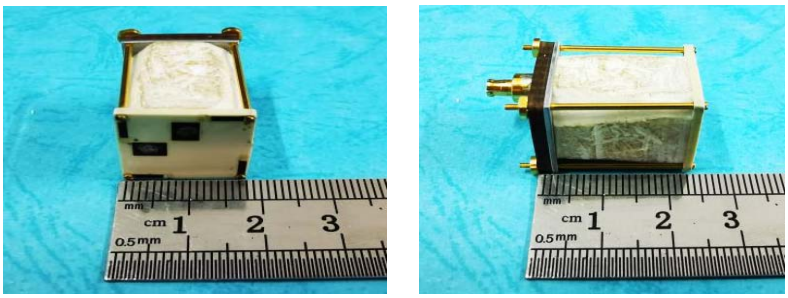

Figure 10. Photograph of the proposed antenna.

Figure 11 depicts the measured and simulated return losses against frequency for the proposed CP antenna. Within the whole band from 1.2 GHz to 1.35 GHz, both the measured and simulated return losses are below −10 dB. And the resonant frequency is coincident at 1.27 GHz with proper adjustments when the antenna is under test. The slight difference between the two results is mainly because the air gap was not considered in the simulation, and the lossy foam was used to replace the air gap during assembly.

As the shorting pins and parasitic strips are placed symmetrically, the proposed antenna has good axisymmetric radiation patterns. Therefore, only the radiation pattern of $\varphi = 0°$ plane at 1.268 GHz is depicted in Fig. 12. As seen, the radiation patterns have been normalized and have broad beamwidth characteristic, where the HPBW is wider than 140° for both measured and simulated results. For the proposed antenna, the axial ratio (AR) of the boresight against frequency is one of the key indicators. The AR value is measured in the anechoic chamber from 1.248 to 1.288 GHz with 5 MHz interval. As

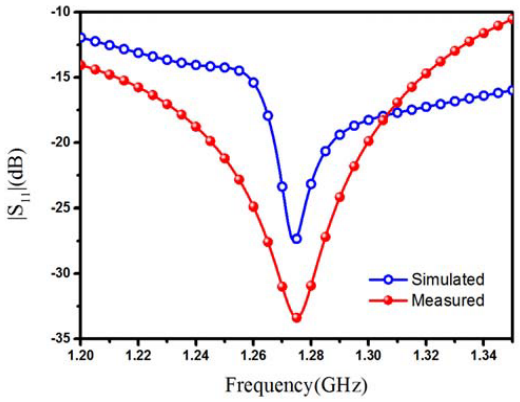

Figure 11. Measured and simulated return loss against frequency.

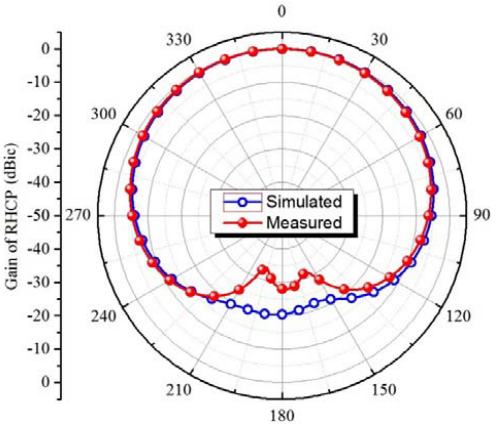

Figure 12. Measured and simulated radiation patterns at 1.268 GHz.

presented in Fig. 13, the simulated AR is below 2 dB within the whole operation band, and the measured AR is varied from 1.16 dB to 1.86 dB. The measured result agrees well with the simulated one.

The measured and simulated peak gains at the boresight are depicted in Fig. 14. Over the B3 operating band of 1268.52 ± 10.23 MHz, the measured RHCP gain is varied from -35 dBic to 0.2 dBic. The measured cross polarization level deteriorates at the higher band. A slight disagreement between the simulated and measured results can be observed, and this discrepancy may be caused by the measuring error, partly due to the unpredictable material tolerance in the microwave substrate.

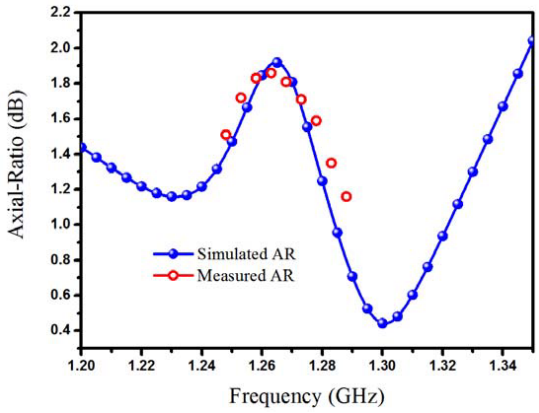

Figure 13. Measured and simulated boresight AR against frequency.

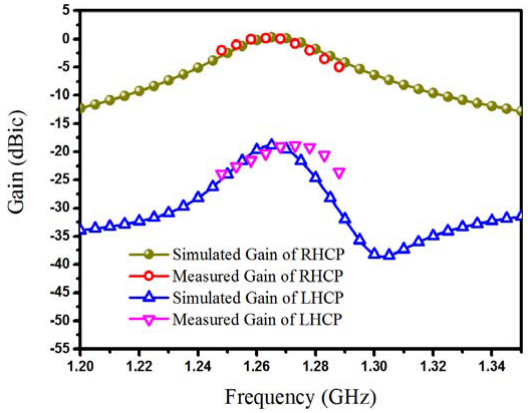

Figure 14. Measured and simulated peak gain at the boresight against frequency.

4. CONCLUSION

In this paper, a novel miniaturized CP antenna for BDS applications has been proposed, investigated, and measured. A considerable small volume about $0.08\lambda_0 \times 0.08\lambda_0 \times 0.1\lambda_0$ has been achieved by these shorting pins and parasitic strips integrated symmetrically, and its weight is about 25 grams. The simulated and measured results have been verified, and a good agreement has been achieved between the two. The proposed antenna achieves below -10 dB for return loss and below 2 dB for AR within the operation band. It also exhibits an enhanced HPBW about 140°. These features such as miniaturized volume, hemispherical radiation pattern, excellent impedance matching, and AR make this antenna a good potential candidate for the BDS applications.

REFERENCES

1. Li, X., X. Zhang, X. Ren, et al., "Precise positioning with current multi-constellation Global Navigation Satellite Systems: GPS, GLONASS, Galileo and BeiDou," *Scientific Reports*, 2015, Doi: 10.1038/srep08328.
2. Zheng, K.-K. and Q.-X. Chu, "A small symmetric slit shaped and annular slotted BeiDou antenna with stable phase center," *IEEE Antennas Wireless Propag. Lett.*, Vol. 17, 146–149, 2018.
3. Shi, H., J. Shi, J. Li, et al., "Miniaturized circularly polarized patch antenna using coupled shorting strip and capacitive probe feed," *International Journal of Electronics and Communications*, Vol. 98, 235–240, 2019.
4. He, M., X.-H. Ye, P.-Y. Zhou, et al., "A small-size dual-feed broadband circularly polarized U-slot patch antenna," *IEEE Antennas Wireless Propag. Lett.*, Vol. 14, 898–901, 2015.
5. Ferreira, R., J. Joubert, and J. W. Odendaal, "A compact dual-circularly polarized cavity-backed ring-slot antenna," *IEEE Trans. Antennas Propagat.*, Vol. 65, 364–368, 2017.
6. Ameen, M. and R. K. Chaudhary, "Metamaterial-based wideband circularly polarised antenna with rotated V-shaped metasurface for small satellite applications," *Electronics Letters*, Vol. 55, 365–366, 2019.
7. Huang, Y.-H., Y. Wang, Y.-L. Zou, and J.-L. Guo, "A miniature circularly polarized air-borne antenna with wide angle coverage," *IEEE Antennas Wireless Propag. Lett.*, Vol. 16, 497–500, 2017.
8. Li, R.-Q., Y.-X. Guo, B. Zhang, and G.-H. Du, "A miniaturized circularly polarized implantable annular-ring antenna," *IEEE Antennas Wireless Propag. Lett.*, Vol. 16, 2566–2569, 2017.
9. Luo, Y., Q.-X. Chu, and L. Zhu, "A miniaturized wide-beamwidth circularly polarized planar antenna via two pairs of folded dipoles in a square contour," *IEEE Trans. Antennas Propagat.*, Vol. 63, 3753–3759, 2015.
10. Lin, W. and R. W. Ziolkowski, "Electrically small, low-profile, huygens circularly polarized antenna," *IEEE Trans. Antennas Propagat.*, Vol. 66, 636–643, 2018.
11. Zhang, B.-C., C. Jin, and Z.-X. Shen, "Low-profile broadband absorber based on multimode resistor-embedded metallic strips," *IEEE Trans. Microw. Theory Techn.*, 1–9, 2019.
12. Reddy, V. V., N. V. S. N. Sarma, "Compact circularly polarized asymmetrical fractal boundary microstrip antenna for wireless applications," *IEEE Antennas Wireless Propag. Lett.*, Vol. 13, 118–121, 2014.
13. So, K. K., H. Wong, K. M. Luk, and C.-H. Chan, "Miniaturized circularly polarized patch antenna with low back radiation for GPS satellite communications," *IEEE Trans. Antennas Propagat.*, Vol. 63, 5934–5938, 2015.
14. Gupta, S. and G. Mumcu, "Circularly polarised printed antenna miniaturised using complementary split-ring resonators and reactive pin loading," *IET Microw. Antennas & Propaga.*, Vol. 9, 118–124, 2019.
15. Sun, C., H.-L. Zheng, and Y. Liu, "Analysis and design of a low-cost dual-band compact circularly polarized antenna for GPS application," *IEEE Trans. Antennas Propagat.*, Vol. 64, 365–370, 2016.
16. Wong, H., K. K. So, K. B. Ng, et al., "Virtually shorted patch antenna for circular polarization," *IEEE Antennas Wireless Propag. Lett.*, Vol. 9, 1213–1216, 2010.
17. Liao, S.-W. and Q. Xue, "Miniaturized VHF/UHF dual-band circularly polarized four-element sequential-rotation array antenna based on alternately overlapped bent radiation-coupled dual-L antenna elements," *IEEE Trans. Antennas Propagat.*, Vol. 66, 4924–4929, 2018.
18. Juan, Y., W.-C. Yang, and W.-Q. Che, "Miniaturized low-profile circularly polarized metasurface antenna using capacitive loading," *IEEE Trans. Antennas Propagat.*, Vol. 67, 3527–3532, 2019.
19. Liu, C.-R., Y.-D. Zhang, and X.-G. Liu, "Circularly polarized implantable antenna for 915 MHz ISM-band far-field wireless power transmission," *IEEE Antennas Wireless Propag. Lett.*, Vol. 17, 373–376, 2018.